

# Fuzzy Logic Based Solar Pv-Powered SRM Drive For Evs With Flexible Energy Control Functions

<sup>1</sup> N.V.A.Bhavani <sup>2</sup> P.Sanjeev Kumar

<sup>1</sup> Assistant Professor of Electrical and Electronics Engineering, S.R.K.R. Engineering College

<sup>2</sup> M.Tech Scholar, Electrical and Electronics Engineering, S.R.K.R. Engineering College

## ABSTRACT

In this thesis we are proposing new approach is fuzzy logic control for Electric vehicles (EVs) provide a feasible solution to reduce greenhouse gas emissions and thus become a hot topic for research and development. Switched reluctance motors (SRMs) are one of the promised motors for EV applications. In order to extend the EVs' driving miles, the use of photovoltaic (PV) panels on the vehicle helps to decrease the reliance on vehicle batteries. Based on the phase winding characteristics of SRMs, a tri-port converter is proposed in this paper to control the energy flow among the PV panel, battery, and SRM. Six operating modes are presented, four of which are developed for driving and two for standstill on board charging by fuzzy logic. In the driving modes, the energy decoupling control for maximum power point tracking (MPPT) of the PV panel and speed control of the SRM are realized. In the standstill charging modes, a grid-connected charging topology is developed without a need for external hardware. When the PV panel directly charges the battery, a multi section charging control strategy is used to optimize energy utilization using fuzzy logic. Simulation results based on MATLAB/Simulink prove the effectiveness of the proposed tri-port converter, which have potential economic implications to improve the market acceptance of EV.

## INTRODUCTION

ELECTRIC vehicles (EVs) have taken a significant leap forward by advances in motor drives, power converters, batteries, and energy management systems [1]–[4]. However, due to the limitation of current battery technologies, the driving miles are relatively short that restricts the wide application of

EVs [5]–[7]. In terms of motor drives, high-performance permanent-magnet (PM) machines are widely used while rare earth materials are needed in large quantities, limiting the wide application of EVs [8], [9]. In order to overcome these issues, a photovoltaic (PV) panel and a switched reluctance motor (SRM) are introduced to provide power supply and motor drive, respectively. First, by adding the PV panel on top of the EV, a sustainable energy source is achieved. Nowadays, a typical passenger car has a surface enough to install a 250-W PV panel [10]. Second, a SRM needs no rare-earth PMs and is also robust so that it receives increasing attention in EV applications [11]–[16]. While PV panels have low-power density for traction drives, they can be used to charge batteries most of time. Generally, the PV-fed EV has a similar structure to the hybrid electrical vehicle (HEV), whose internal combustion engine (ICE) is replaced by the PV panel. The PV-fed EV system is illustrated in Fig. 1. Its key components include an off-board charging station, a PV, batteries, and power converters [17]–[19]. In order to decrease the energy conversion processes, one approach is to redesign the motor to include some onboard charging functions [20]–[22]. For instance, paper [22] designs a 20-kW split-phase PM motor for EV charging, but it suffers from high harmonic contents in the back electromotive force (EMF). Another solution is based on a traditional SRM. Paper [23] achieves onboard charging and power factor correction in a 2.3-kW SRM by employing machine windings as the input filter inductor. The concept of modular structure of driving topology is proposed in paper [24]. Based on the intelligent power modules (IPMs), a four-phase half bridge converter is employed to achieve driving and grid-charging. Although modularization supports mass production, the use of half/full bridge topology reduces the system reliability (e.g., shoot-through issues). Paper [25] develops a simple topology for

plug-in HEV that supports flexible energy flow. But for grid-charging, the grid should be connected to the generator rectifier that increases the energy conversion process and decreases the charging efficiency. Nonetheless, an effective topology and control strategy for PV-fed EVs is not yet developed. Because the PV has different characteristics to ICEs, the maximum power point tracking (MPPT) and solar energy utilization are the unique factors for the PV-fed EVs.

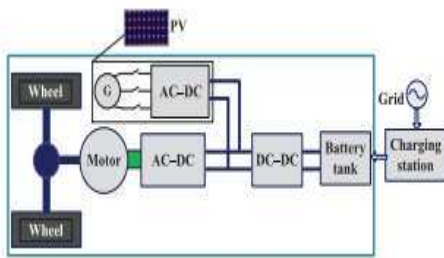


Fig. 1. PV-fed HEV.

absorbs the photon energy from the sun and converts it into electricity using the photovoltaic (PV) effect principle. Thin-film or silicon material are used in the manufacturing of PV modules. This will provide approximately constant power at low cost and also it is pollution free. A general PV cell produces maximum of 3 watts with nearly 1/2V dc. Number of PV cells connected in series or parallel to make a PV module.

## II. SOLAR CELL CHARACTERISTICS

The solar cell is mainly made of PV wafers, converts the light energy of solar irradiation into voltage and current directly for load, and conducts electricity without electrolytic effect. The electric energy is obtained from the PN interface of semiconductor directly; therefore, the solar cell is also known as PV cell. The equivalent circuit of solar cell as shown in Figure 2.

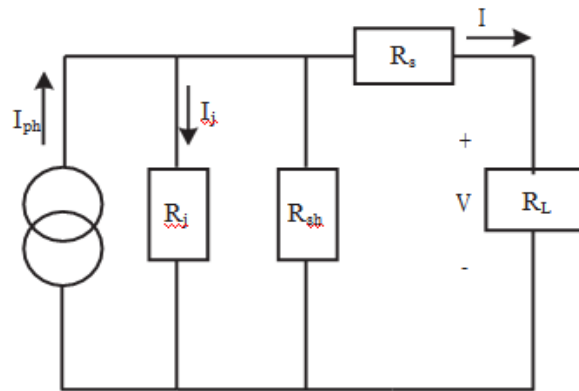


Fig. 2 Equivalent circuit of PV array

The current source  $I_{ph}$  represents the cell photovoltaic current,  $R_j$  is used to represent the nonlinear resistance of the p-n junction,  $R_{sh}$  and  $R_s$  are used to represent the intrinsic shunt and series resistance respectively. Normally value of  $R_{sh}$  is very large and  $R_s$  is very small. Hence both of them can be neglected to simplify the analysis. PV cells are grouped in larger units to form PV modules. They are further interconnected in series-parallel combination to form PV arrays. The mathematical model used to simplify the PV array is represented by the equation

$$I = n_p I_{ph} - n_p I_{rs} \left[ e^{\left( \frac{q}{kTA} \cdot \frac{V}{n_s} \right)} - 1 \right]$$

Where  $I$  is the PV array output current,  $V$  is the PV array output voltage,  $n_s$  is the number of series cells,  $n_p$  is the number of parallel cells,  $q$  is the charge of an electron,  $k$  is the Boltzmann constant,  $A$  is the p-n junction ideality factor,  $T$  is the cell temperature, and  $I_{rs}$  is the cell reverse saturation current. The factor  $A$  decides the deviation of solar cell from the ideal p-n junction characteristics. Its value ranges from one to five. The photo current  $I_{ph}$  depends on the solar irradiance and cell temperature as below

$$I_{ph} = [I_{scr} + K_i(T - T_r)] \frac{S}{100}$$

Where  $I_{scr}$  is the cell short circuit current at reference temperature and radiation,  $K_i$  is the short circuit current temperature coefficient and  $S$  is the solar irradiance in mW/cm<sup>2</sup>. The Simulink model of PV array is shown in Fig. 4. The model includes three

subsystems. One subsystem to model PV module and two more subsystems to model  $I_{ph}$  and  $I_{rs}$

### Perturb and Observe MPPT Algorithm for PV array

Perturb and Observe (known as P&O) algorithm, shown in Fig .9, is used in this paper for maximum power tracking of PV array. This method involves perturbation of the voltage,  $V$ , and observing the change in power output,  $P$ . If the perturbation in one direction increases the power output of the PV array, then the same direction of perturbation is continued. Otherwise, the direction of perturbation is reversed. Thus, it is a continuous process of searching for the voltage on power  $V$  vs voltage (P-V) curve, which increases the power output of the PV array. This method is well described in the literature [12], hence, not explained here in detail.

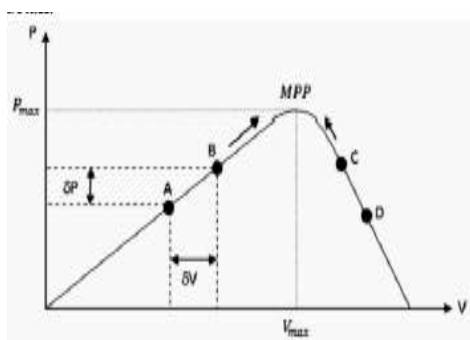


**Figure 3. Description of P&O algorithm for MPPT**

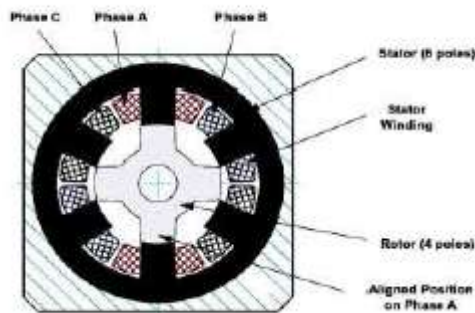
### SRM DRIVE

The switched reluctance motor (SRM) is a type of motor doubly salient with phase coils mounted around diametrically opposite stator poles. There are no windings or permanent magnets on the rotor. The rotor is basically a piece of (laminated) steel and its shape forms salient poles. The stator has concentrated coils. Switched reluctance motors (SRM) have a simple and robust structure, thus they are generally suitable for high-speed applications. High-speed motors have the advantage of high power density, which is an important issue of traction motors in

electric vehicles (EV). Therefore, high speed SRM seems to be promising candidates for this application.

### 2.2 SRM PRINCIPLE OF OPERATION

SRM differ in the number of phases wound on the stator. Each of them has a certain number of suitable combinations of stator and rotor poles. Figure 2.5 illustrates a typical 3-Phase SRM with a six stator / four rotor pole configuration. The rotor of an SRM is said to be at the aligned position with respect to a fixed phase if the current reluctance has the minimum value (Corda et al 1979); and the rotor is said to be in the unaligned position with respect to a fixed phase if the current reluctance reaches its maximum value. The motor is excited by a sequence of current pulses applied at each phase. The individual phases are consequently excited, forcing the motor to rotate. The current pulses must be applied to the respective phase at the exact rotor position relative to the excited phase. When any pair of rotor poles is exactly in line with the stator poles of the selected phase, the phase is said to be in an aligned position; i.e., the rotor is in the position of maximum stator inductance (Figure 4).



#### A. Proposed Topology and Working Modes

The proposed tri-port topology has three energy terminals, PV, battery, and SRM. They are linked by a power converter that consists of four switching devices ( $S_0 - S_3$ ), four diodes ( $D_0 - D_3$ ), and two relays, as shown in Fig. 2 [26]. By controlling relays  $J_1$  and  $J_2$ , the six operation modes are supported, as shown in Fig. 3; the corresponding relay actions are illustrated in Table I. In mode 1, PV is the energy

source to drive the SRM and to charge the battery. In mode 2, the PV and battery are both the energy sources to drive the SRM. In mode 3, the PV is the source and the battery is idle. In mode 4, the battery is the driving source and the PV is idle. In mode 5, the battery is charged by a singlephase grid while both the PV and SRM are idle. In mode 6, the battery is charged by the PV and the SRM is idle.

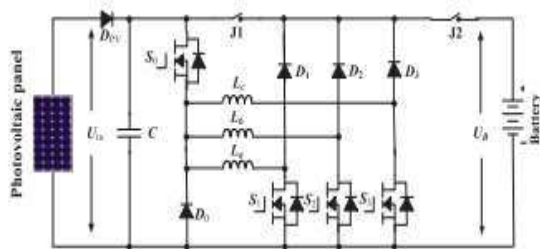


**Fig.5.** Proposed tri-port topology for PV-powered SRM drive.

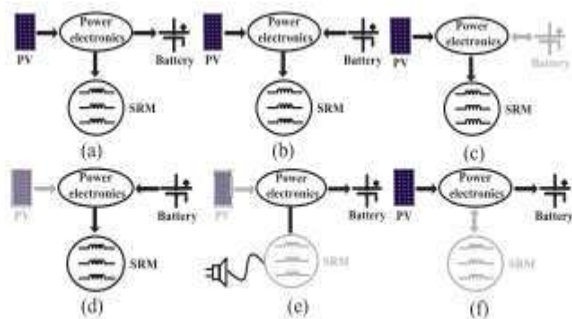


**Fig.6.** Six operation modes of the proposed tri-port topology. (a) Mode 1. (b) Mode 2. (c) Mode 3. (d) Mode 4. (e) Mode 5. (f) Mode 6.

## B. Driving Modes

Operating modes 1–4 are the driving modes to provide traction drive to the vehicle.

1) Mode 1: At light loads of operation, the energy generated from the PV is more than the SRM needed; the system operates in mode 1. The corresponding operation circuit is shown in Fig. 4(a), in which relay J1 turns off and relay J2 turns on. The PV panel energy feeds the energy to SRM and charges the

battery; so in this mode, the battery is charged in EV operation condition.

2) Mode 2: When the SRM operates in heavy load such as uphill driving or acceleration, both the PV panel and battery supply power to the SRM. The corresponding operation circuit is shown in Fig. 4(b), in which relay J1 and J2 are turned on.

3) Mode 3: When the battery is out of power, the PV panel is the only energy source to drive the vehicle. The corresponding circuit is shown in Fig. 4(c). J1 turns on and J2 turns off.

4) Mode 4: When the PV cannot generate electricity due to low solar irradiation, the battery supplies power to the SRM. The corresponding topology is illustrated in Fig. 4(d). In this mode, relay J1 and J2 are both conducting.

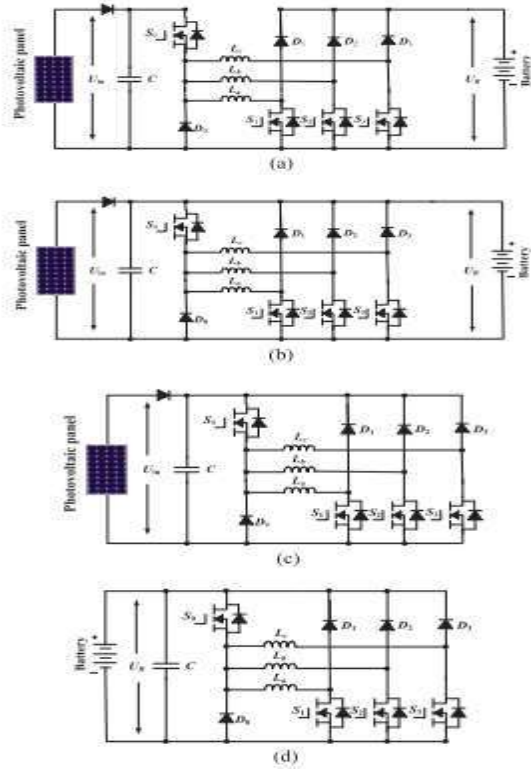


**Fig: 7.** Equivalent circuits under driving modes. (a) Operation circuit under mode 1. (b) Operation circuit under mode 2. (c) Operation circuit under mode 3. (d) Operation circuit under mode 4.

### C. Battery Charging Modes

Operating modes 5 and 6 are the battery charging modes.

5) Mode 5: When PV cannot generate electricity, an external power source is needed to charge the battery, such as ac grid. The corresponding circuit is shown in Fig. 5(a). J1 and J2 turn on. Point A is central tapped of phase windings that can be easily achieved without changing the motor structure. One of the three-phase windings is split and its midpoint is pulled out, as shown in Fig. 5(a). Phase windings La1 and La2 are employed as input filter inductors. These inductors are part of the drive circuit to form an ac-dc rectifier for grid-charging.

6) Mode 6: When the EV is parked under the sun, the PV can charge the battery. J1 turns off and J2 turns on. The corresponding charging circuit is shown in Fig. 5(b).

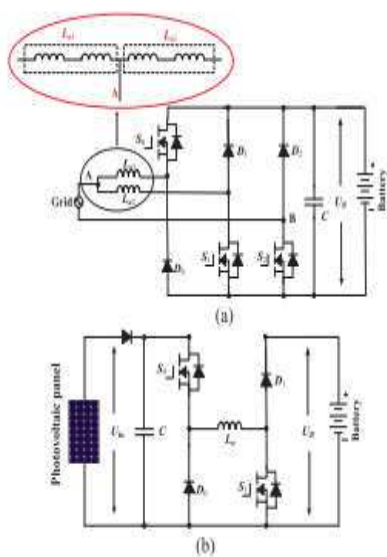


**Fig: 8.** Equivalent circuits of charging condition modes. (a) Grid charging mode. (b) PV source charging mode.

### FUZZY LOGIC

Fuzzy logic theory is seen as one of the most successful of today's technologies for developing sophisticated control systems. The reason for which is very simple as it resembles human decision making with an ability to generate precise solutions from approximate information. Fuzzy design can accommodate the ambiguities of real-world human language and logic where as other approaches require exact equations to model real-world behaviors of the system. The fuzzy logic fills vital gap in engineering design methods left vacant by purely mathematical approaches and purely logic-based approaches

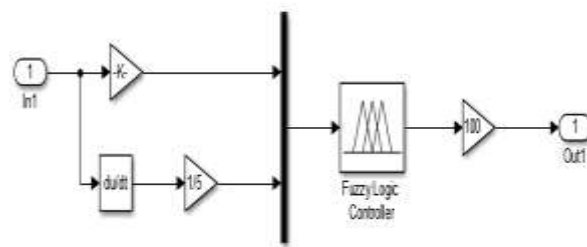


**Fig 9 :** simulation of proposed fuzzy logic converter

Fuzzy logic control includes establishing a fuzzy inference system with the input and output membership functions and defining the rules related to it. Here, we have two input membership functions :1)Error in output voltage- "error" and 2)Changing error- "delta error". The only output membership function is the duty cycle- "output1". The input membership functions "error", "delta error" and output membership function "output1" is shown in fig. 7.

	NB	NM	NS	ZE	PS	PM	PB
NB	NB	NB	NB	NB	NM	NS	ZE
NM	NB	NB	NB	NM	NS	ZE	PS
NS	NB	NB	NM	NS	ZE	PS	PM
ZE	NB	NM	NS	ZE	PS	PM	PB
PS	NM	NS	ZE	PS	PM	PB	PB
PM	NS	ZE	PS	PM	PB	PB	PB
PB	ZE	PS	PM	PB	PB	PB	PB

Fig10 . Fuzzy rules

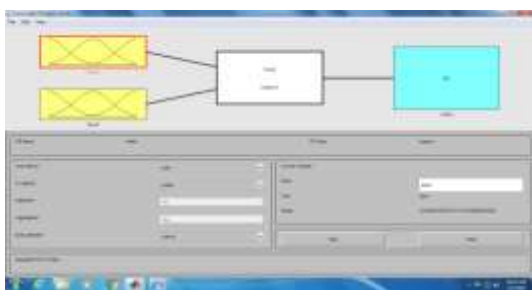


Fig 11: Inputs of fuzzy logic controller

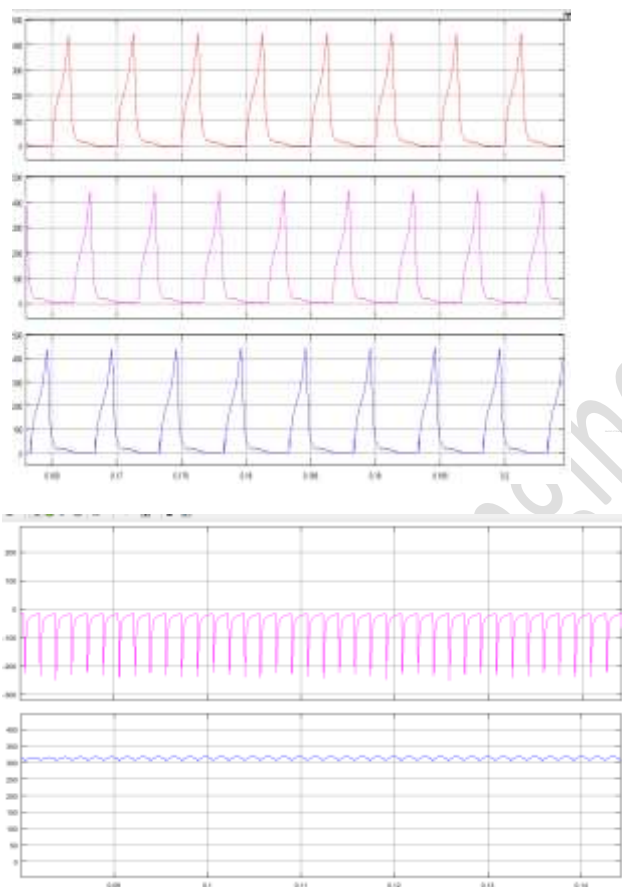


Fig. 12A . Simulation results for driving conditions at modes 1, 3, and 4. (a) Simulation results of driving-charging mode (mode 1).

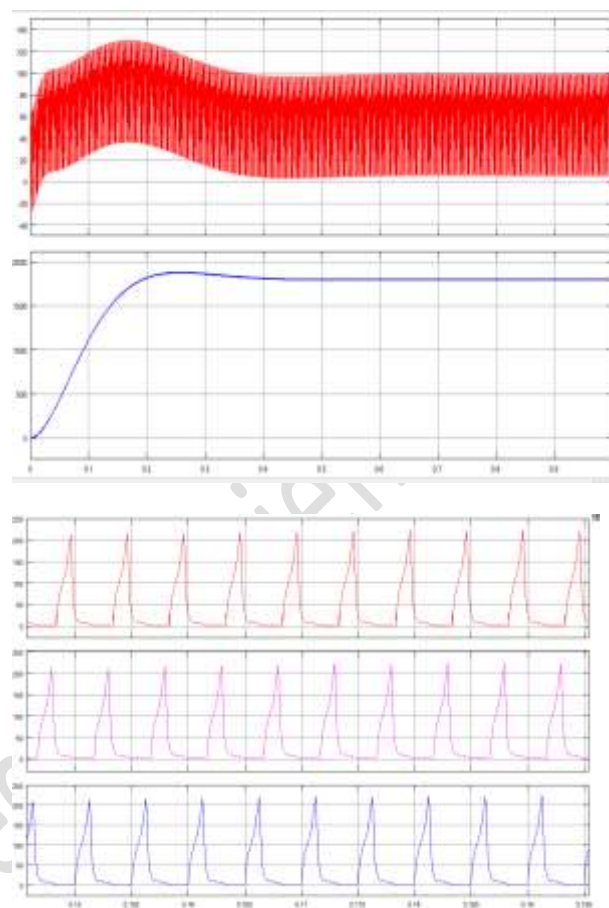
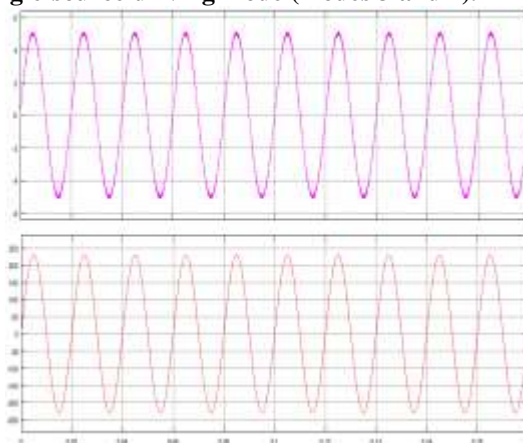
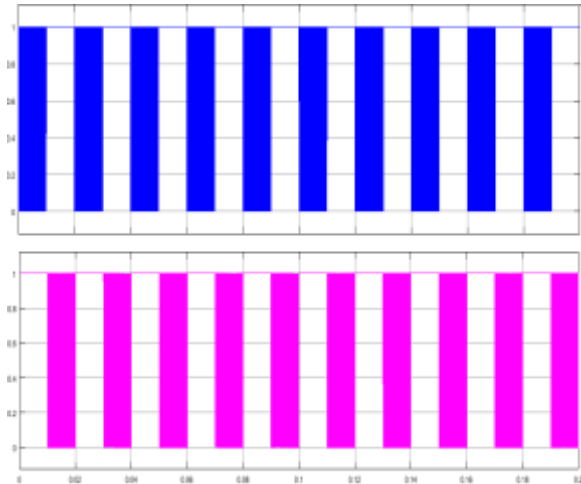
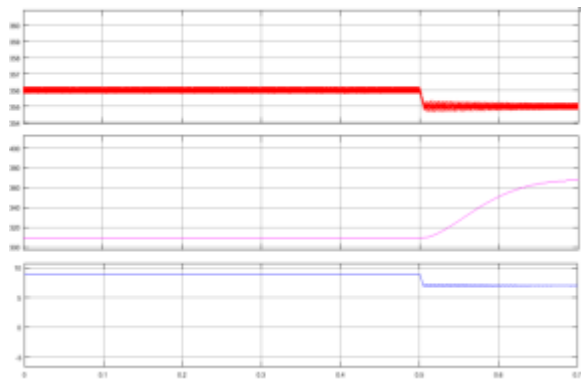


Fig. 12B . Simulation results for driving conditions at modes 1, 3, and 4. (b) Simulation results of single-source driving mode (modes 3 and 4).





**Fig. 13A . Simulation results for charging modes.  
(a) Grid charging (mode 5).**



**Fig. 13B. Simulation results for charging modes  
b) PV charging mode 6 (stages 1-2).**

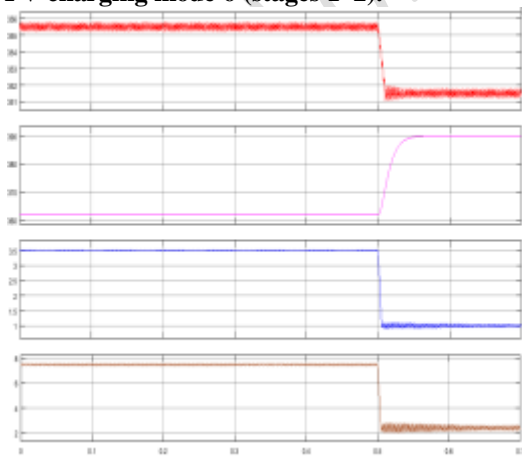


**Fig. 13C. Simulation results for charging  
modes (c) PV charging mode 6 (stages 2-3).**

## CONCLUSION

In order to tackle the range anxiety of using EVs and decrease the system cost, a combination of the PV panel and SRM is proposed as the EV driving system with fuzzy system. The main contributions of this paper are as follows. 1) A tri-port converter is used to coordinate the PV panel, battery, and SRM with fuzzy. 2) Six working modes are developed to achieve flexible energy flow for driving control, driving/charging hybrid control, and charging control with fuzzy. 3) A novel grid-charging topology is formed without a need for external power electronics devices with fuzzy. 4) A PVfed battery charging control scheme is developed to improve the solar energy utilization with fuzzy. Since PV-fed EVs are a greener and more sustainable technology than conventional ICE vehicles, this work will provide a feasible solution to reduce the total costs and CO<sub>2</sub> emissions of electrified vehicles. Furthermore, the proposed fuzzy technology may also be applied to similar applications such as fuel cell powered EVs. Fuel cells have a much high-power density and are thus better suited for EV applications.

## REFERENCES

- [1] A. Emadi, L. Young-Joo, and K. Rajashekara, "Power electronics and motor drives in electric, hybrid electric, and plug-in hybrid electric vehicles," *IEEE Trans. Ind. Electron.*, vol. 55, no. 6, pp. 2237–2245, Jun. 2008.
- [2] L. K. Bose, "Global energy scenario and impact of power electronics in 21st century," *IEEE Trans. Ind. Electron.*, vol. 60, no. 7, pp. 2638–2651, Jul. 2013.
- [3] J. De Santiago et al., "Electrical motor drivelines in commercial all-electric vehicles: A review," *IEEE Trans. Veh. Technol.*, vol. 61, no. 2, pp. 475–484, Feb. 2012.
- [4] Z. Amjadi and S. S. Williamson, "Power-electronics-based solutions for plug-in hybrid electric vehicle energy storage and management systems," *IEEE Trans. Ind. Electron.*, vol. 57, no. 2, pp. 608–616, Feb. 2010.
- [5] A. Kuperman, U. Levy, J. Goren, A. Zafransky, and A. Savernin, "Battery charger for electric vehicle

traction battery switch station,” IEEE Trans. Ind. Electron., vol. 60, no. 12, pp. 5391–5399, Dec. 2013.

[6] S. G. Li, S. M. Sharkh, F. C. Walsh, and C. N. Zhang, “Energy and battery management of a plug-in series hybrid electric vehicle using fuzzy logic,” IEEE Trans. Veh. Technol., vol. 60, no. 8, pp. 3571–3585, Oct. 2011.

[7] H. Kim, M. Y. Kim, and G. W. Moon, “A modularized charge equalizer using a battery monitoring IC for series-connected Li-ion battery strings in electric vehicles,” IEEE Trans. Power Electron., vol. 28, no. 8, pp. 3779–3787, May 2013.

[8] Z. Ping, Z. Jing, L. Ranran, T. Chengde, and W. Qian, “Magnetic characteristics investigation of an axial–axial flux compound-structure PMSM used for HEVs,” IEEE Trans. Magn., vol. 46, no. 6, pp. 2191–2194, Jun. 2010.

[9] A. Kolli, O. Béthoux, A. De Bernardinis, E. Labouré, and G. Coquery, “Space-vector PWM control synthesis for an H-bridge drive in electric vehicles,” IEEE Trans. Veh. Technol., vol. 62, no. 6, pp. 2441–2452, Jul. 2013.

[10] Y. Hu, C. Gan, W. Cao, W. Li, and S. Finney, “Central-tapped node linked modular fault tolerance topology for SRM based EV/HEV applications,” IEEE Trans. Power Electron., vol. 31, no. 2, pp. 1541–1554, Feb. 2016.

[11] S. M. Yang and J. Y. Chen, “Controlled dynamic braking for switched reluctance motor drives with a rectifier front end,” IEEE Trans. Ind. Electron., vol. 60, no. 11, pp. 4913–4919, Nov. 2013.

[12] B. Bilgin, A. Emadi, and M. Krishnamurthy, “Comprehensive evaluation of the dynamic performance of a 6/10 SRM for traction application in PHEVs,” IEEE Trans. Ind. Electron., vol. 60, no. 7, pp. 2564–2575, Jul. 2013.

[13] M. Takeno, A. Chiba, N. Hoshi, S. Ogasawara, M. Takemoto, and M. A. Rahman, “Test results and torque improvement of the 50-kW switched reluctance motor designed for hybrid electric vehicles,”